

## **Supplemental Information**

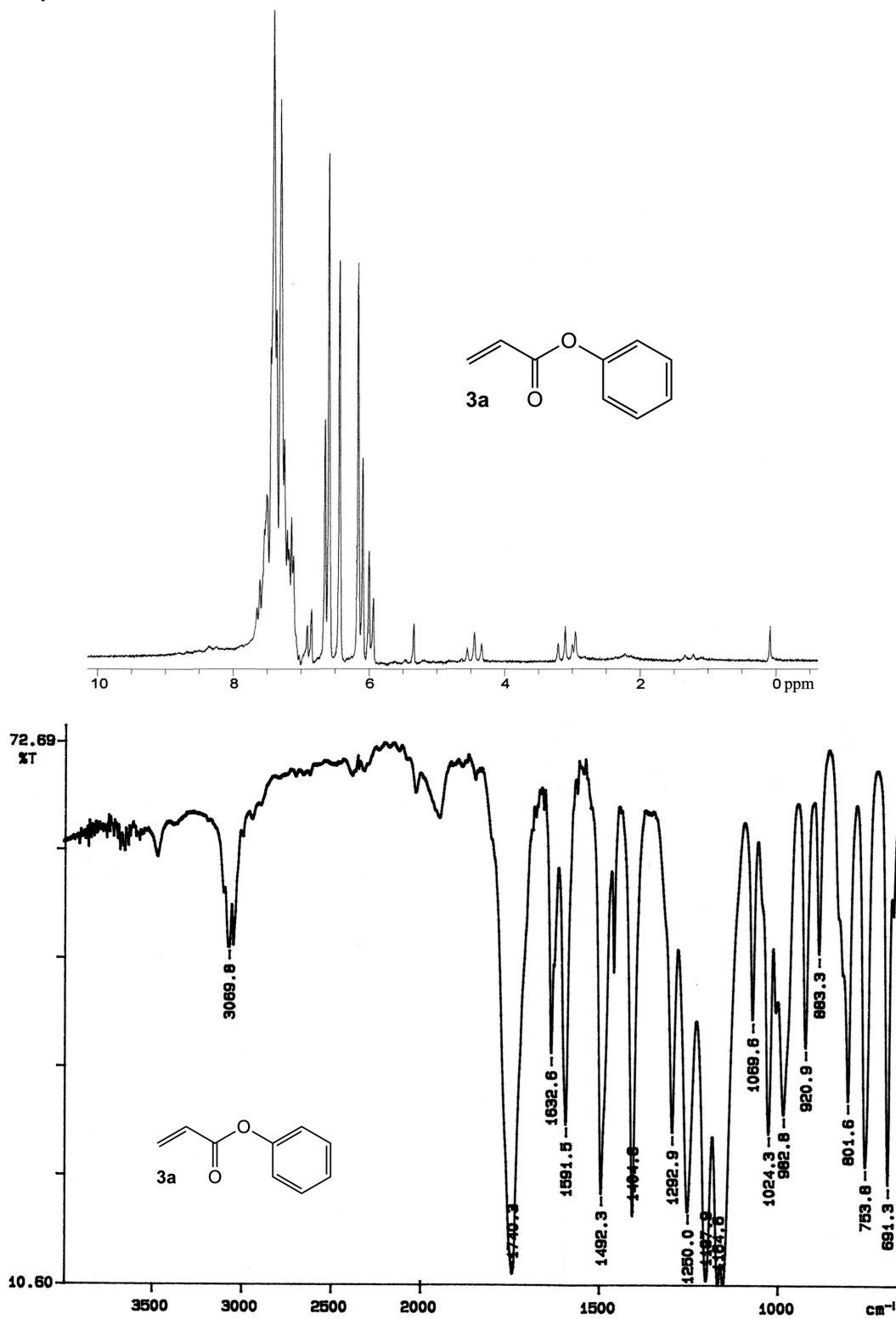
### **Thermodynamic Surface Analyses**

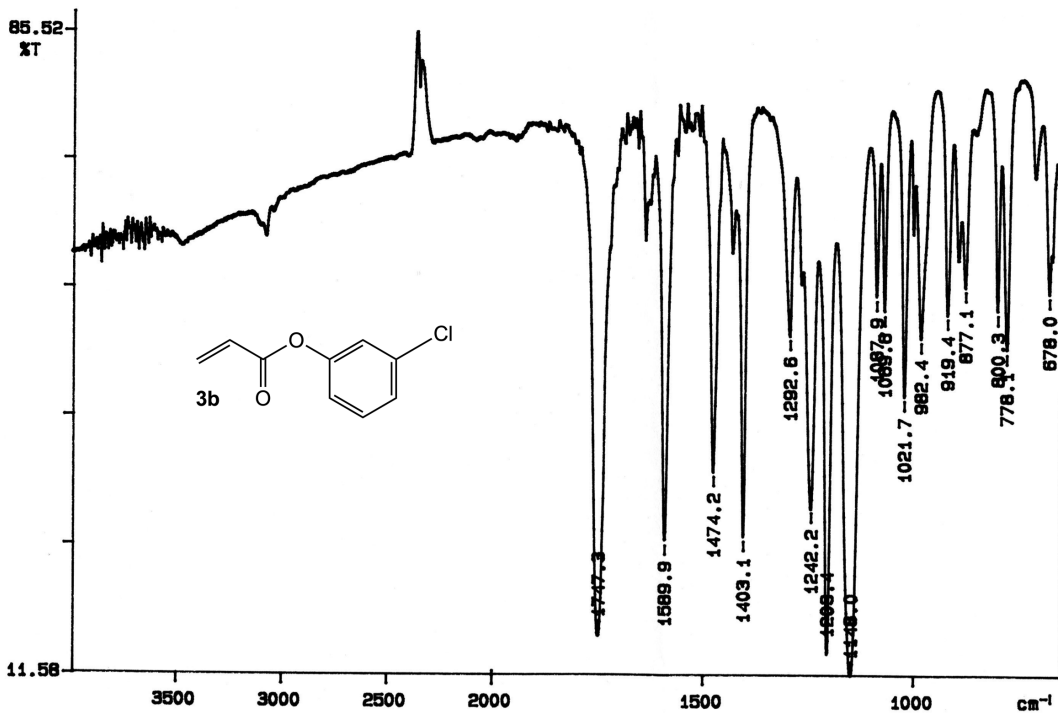
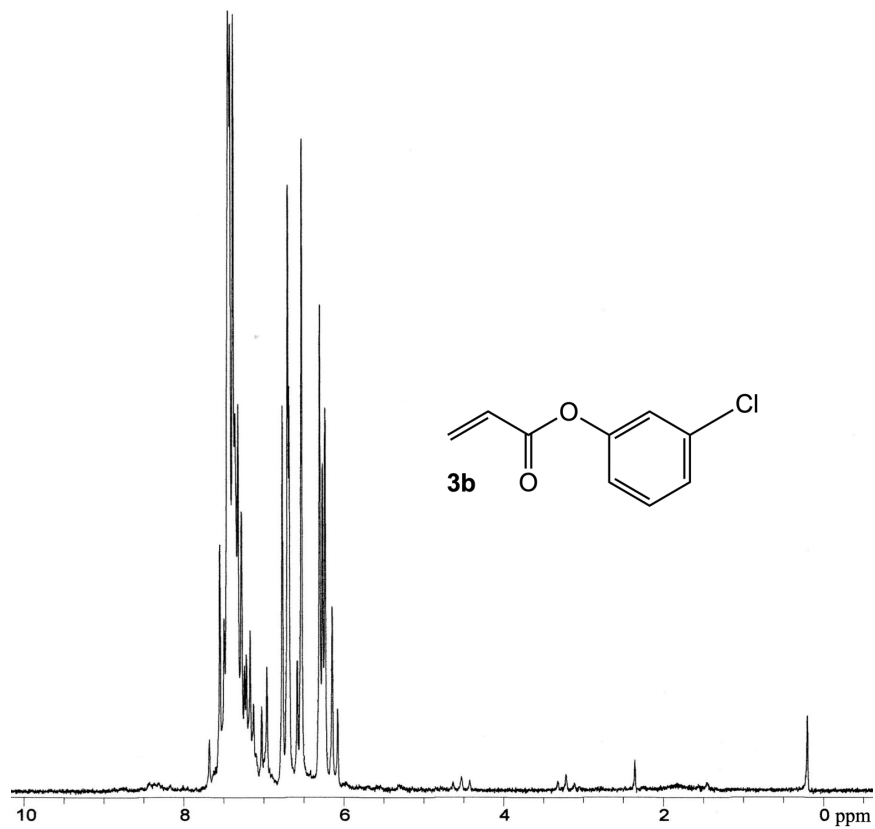
#### **to Inform Biofilm Resistance**

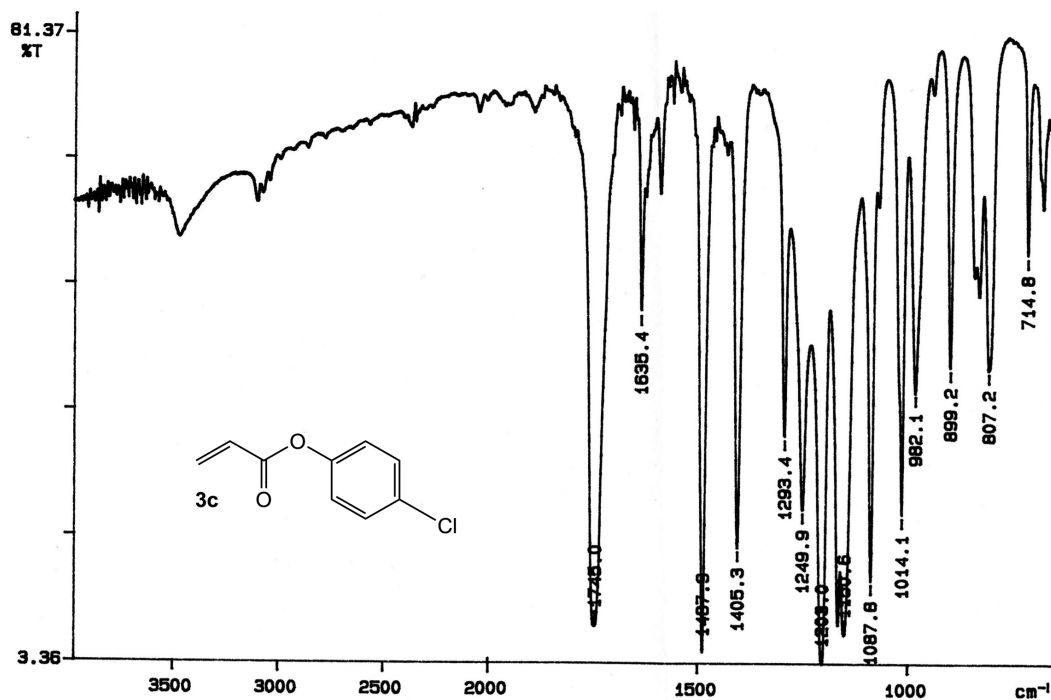
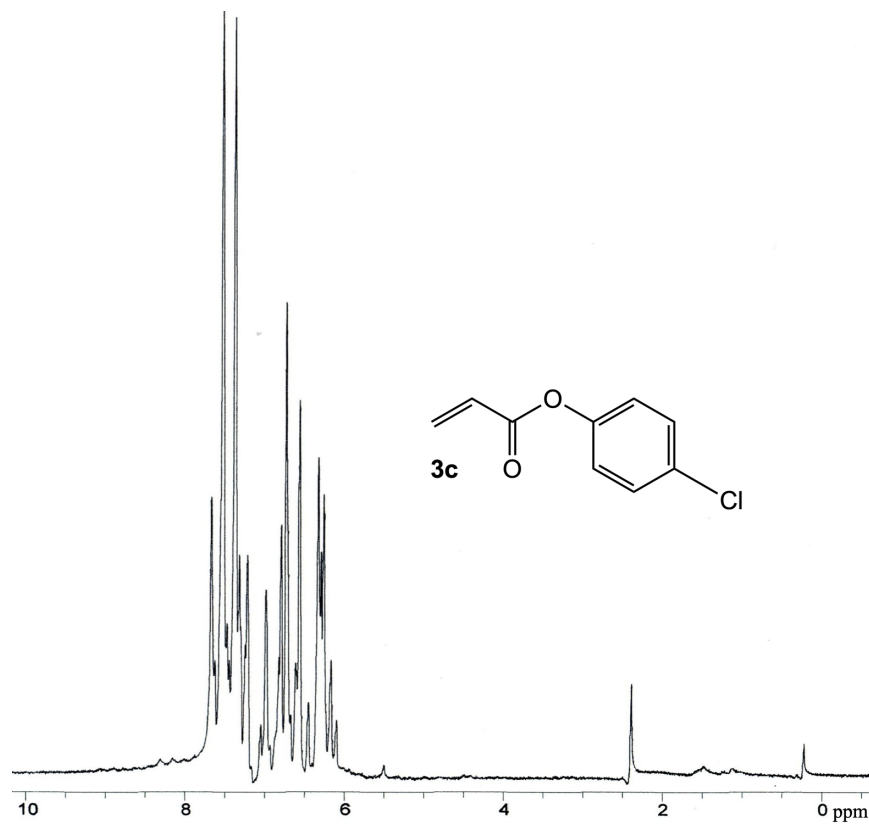
**T. Brian Cavitt, Jasmine G. Carlisle, Alexandra R. Dodds, Rebecca A. Faulkner, Tyson C. Garfield, Verena N. Ghebranious, Phillip R. Hendley, Emily B. Henry, Charles J. Holt, Jordan R. Lowe, Jacob A. Lowry, D. Spencer Oskin, Pooja R. Patel, Devin Smith, and Wenting Wei**

SUPPLEMENTAL INFORMATION

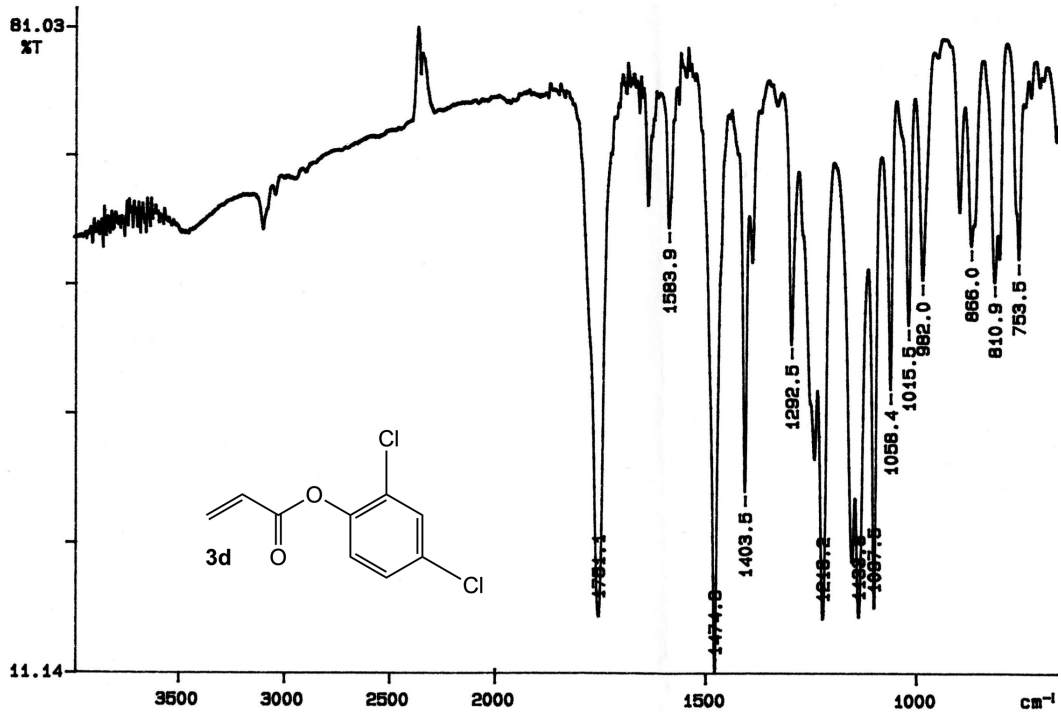
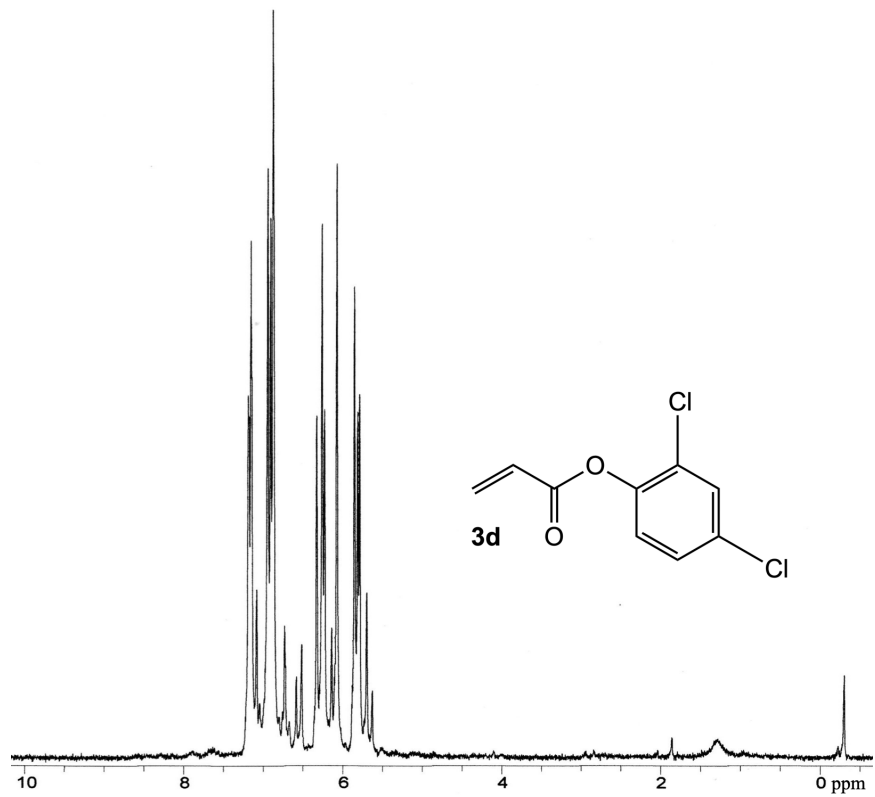
Data S1. Spectra of Products: Related to Table 1.

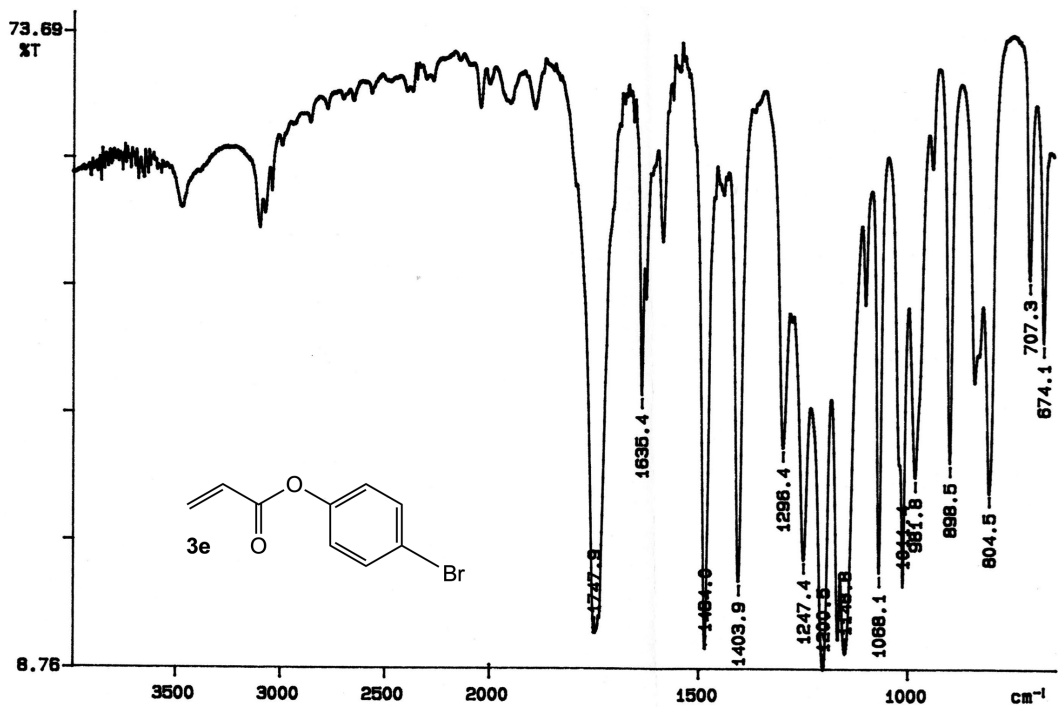
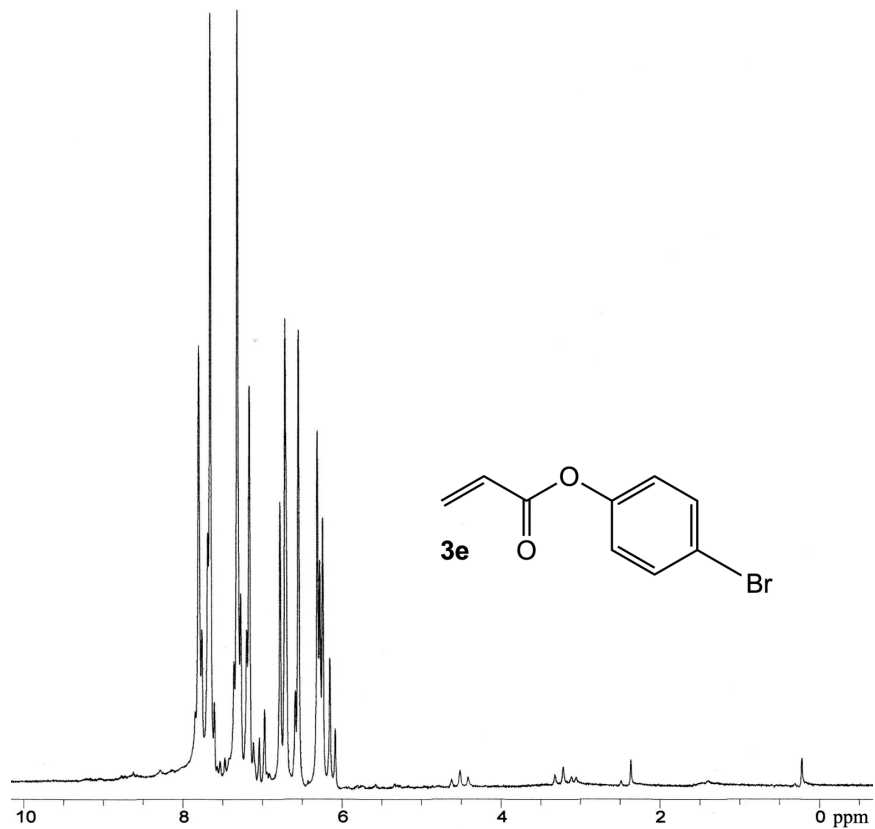


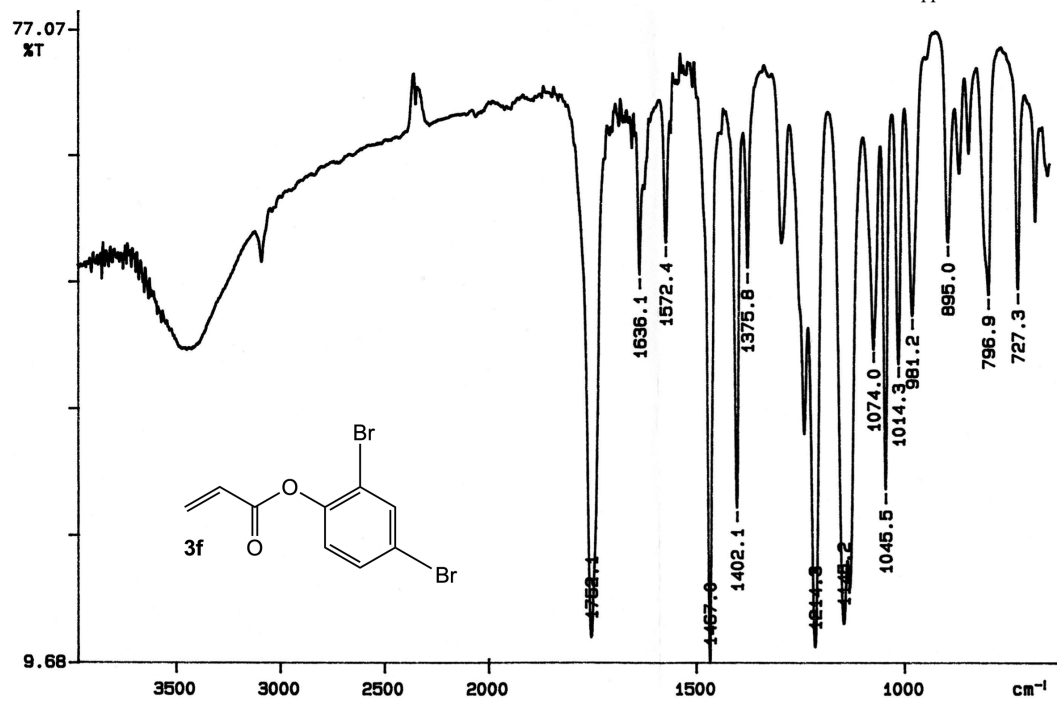
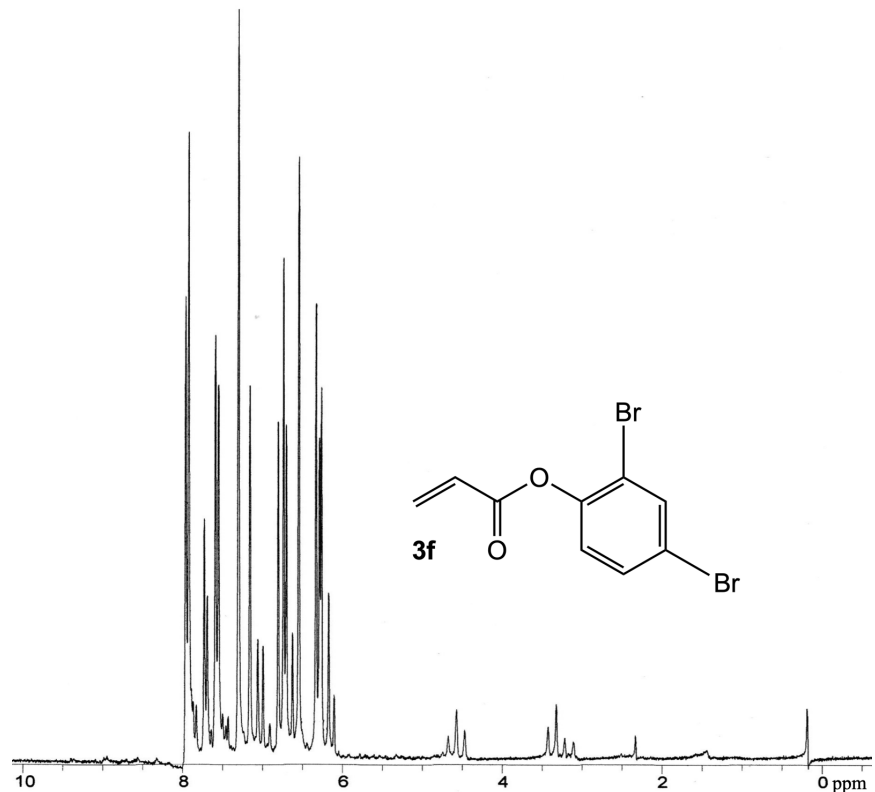


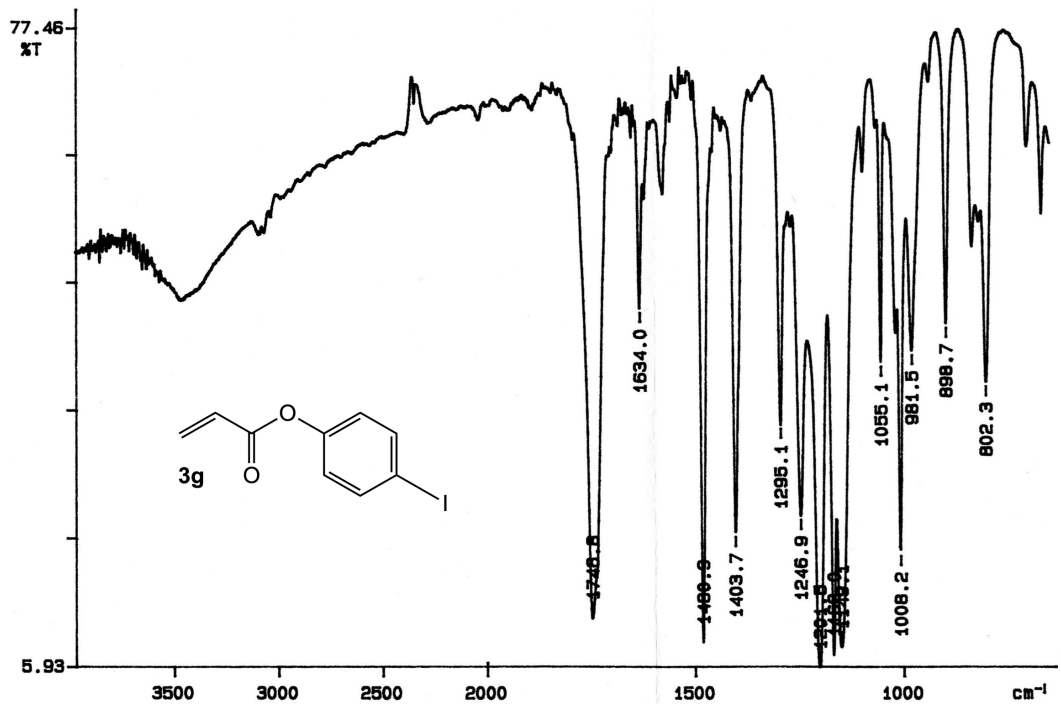
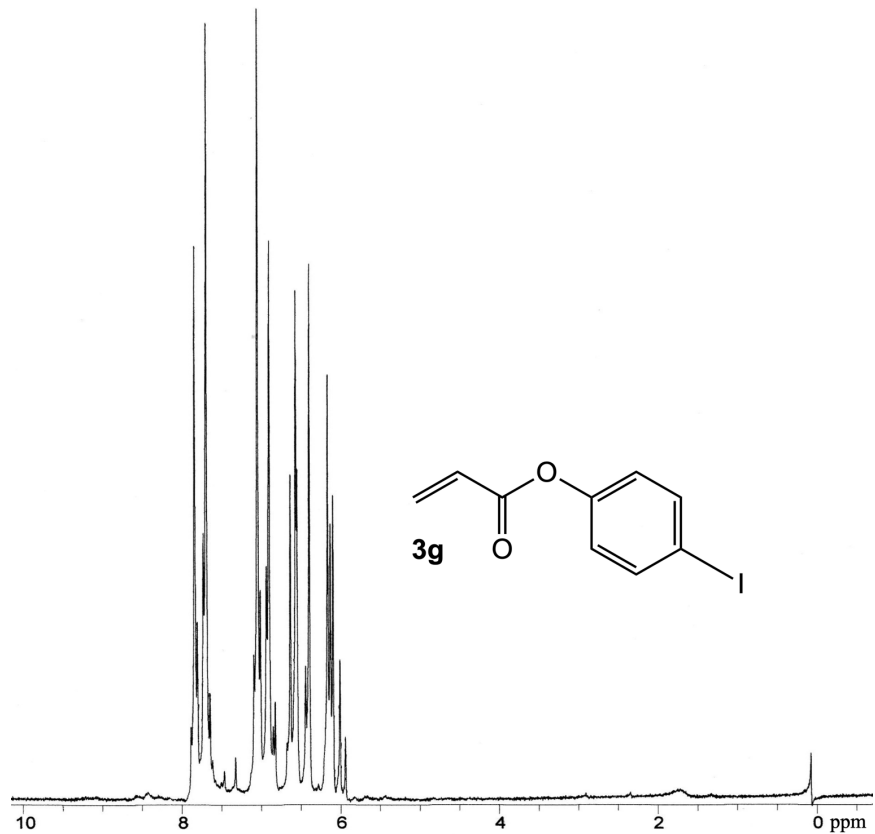






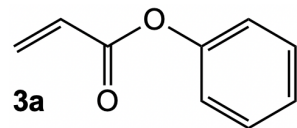






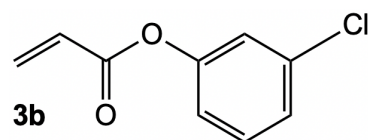
## Data S2. Product Characterization: Related to Table 1.

### Phenyl Acrylate (**3a**).



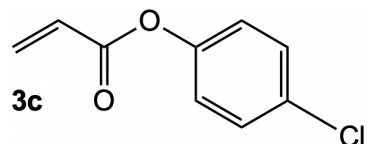
A colorless oil; average isolated yield = 59%;  $n_D^{25} = 1.5354$ ;  $\epsilon_{266\text{ nm}} = 587.18\text{ M}^{-1}\text{cm}^{-1}$ ;  $\epsilon_{313\text{ nm}} = 11.33\text{ M}^{-1}\text{cm}^{-1}$ ;  $\epsilon_{365\text{ nm}} = 4.00\text{ M}^{-1}\text{cm}^{-1}$ ;  $^1\text{H NMR}$  (60 MHz, NEAT)  $\delta$  6.93-7.61 (m, 5H), 5.83-6.59 (m, 3H); IR ( $\nu$ ,  $\text{cm}^{-1}$ ) 1740.3, 1591.5, 1197.9, 982.8, 920.9, 883.3, 691.3; MS ( $m/z$ ) 55, 65, 66, 93, 94.

### 3-Chlorophenyl Acrylate (**3b**).



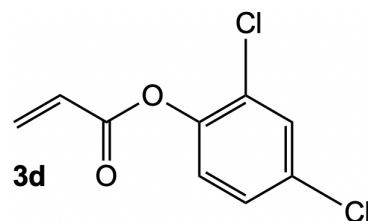
A pale yellow oil; average isolated yield = 33%;  $n_D^{25} = 1.5359$ ;  $\epsilon_{266\text{ nm}} = 761.75\text{ M}^{-1}\text{cm}^{-1}$ ;  $\epsilon_{313\text{ nm}} = 18.74\text{ M}^{-1}\text{cm}^{-1}$ ;  $\epsilon_{365\text{ nm}} = 12.06\text{ M}^{-1}\text{cm}^{-1}$ ;  $^1\text{H NMR}$  (60 MHz, NEAT)  $\delta$  6.71-7.45 (m, 4H), 5.83-6.68 (m, 3H); IR ( $\nu$ ,  $\text{cm}^{-1}$ ) 1747.3, 1589.9, 1209.4, 982.4, 877.1, 778.1, 678.0; MS ( $m/z$ ) 55, 58, 67, 72, 94, 105, 112, 127, 156, 180.

### 4-Chlorophenyl Acrylate (**3c**).



A pale yellow oil; average isolated yield = 36%;  $n_D^{25} = 1.5550$ ;  $\epsilon_{266\text{ nm}} = 454.64\text{ M}^{-1}\text{cm}^{-1}$ ;  $\epsilon_{313\text{ nm}} = 0.42\text{ M}^{-1}\text{cm}^{-1}$ ;  $\epsilon_{365\text{ nm}} = 0.00\text{ M}^{-1}\text{cm}^{-1}$ ;  $^1\text{H NMR}$  (60 MHz, NEAT)  $\delta$  6.92-7.00 (m, 4H), 5.88-6.91 (m, 3H); IR ( $\nu$ ,  $\text{cm}^{-1}$ ) 1745.0, 1635.4, 1203.0, 982.1, 899.2, 807.2; MS ( $m/z$ ) 55, 57, 73, 104, 116, 132, 143, 172.

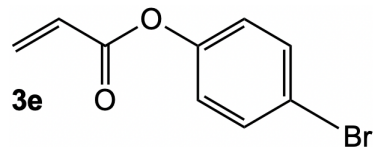
### 2,4-Dichlorophenyl Acrylate (**3d**).



A yellow-orange oil; average isolated yield = 30%;  $n_D^{25} = 1.5900$ ;  $\epsilon_{266\text{ nm}} = 901.33\text{ M}^{-1}\text{cm}^{-1}$ ;  $\epsilon_{313\text{ nm}} = 0.00\text{ M}^{-1}\text{cm}^{-1}$ ;  $\epsilon_{365\text{ nm}} = 0.00\text{ M}^{-1}\text{cm}^{-1}$ ;  $^1\text{H NMR}$  (60 MHz, NEAT)  $\delta$  6.71-7.53 (m, 3H), 5.97-6.61 (m, 3H);

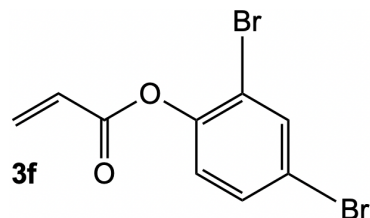
IR ( $\nu$ ,  $\text{cm}^{-1}$ ) 1751.1, 1583.9, 1218.2, 982.0, 875, 866.0  $\text{cm}^{-1}$ , 810.9  $\text{cm}^{-1}$ ; MS ( $m/z$ ) 55, 74, 89, 94, 111, 134, 162, 196, 216, 217, 218, 220.

4-Bromophenyl Acrylate (3e).



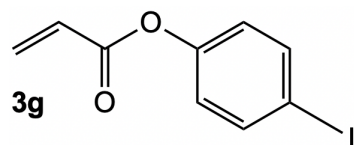
A yellow-orange oil; average isolated yield = 21%;  $n_D^{25} = 1.5580$ ;  $\epsilon_{266\text{ nm}} = 465.11\text{ M}^{-1}\text{cm}^{-1}$ ;  $\epsilon_{313\text{ nm}} = 5.37\text{ M}^{-1}\text{cm}^{-1}$ ;  $\epsilon_{365\text{ nm}} = 0.34\text{ M}^{-1}\text{cm}^{-1}$ ;  $^1\text{H NMR}$  (60 MHz, NEAT)  $\delta$  6.61-7.73 (m, 4H), 5.84-6.58 (m, 3H); IR ( $\nu$ ,  $\text{cm}^{-1}$ ) 1747.9, 1635.4, 1200.5, 981.8, 898.5, 804.5; MS ( $m/z$ ) 50, 55, 73, 98, 109, 133, 162, 216.

2,4-Dibromophenyl Acrylate (3f).



A yellow-orange oil; average isolated yield = 39%;  $n_D^{25} = 1.5998$ ;  $\epsilon_{266\text{ nm}} = 764.62\text{ M}^{-1}\text{cm}^{-1}$ ;  $\epsilon_{313\text{ nm}} = 0.00\text{ M}^{-1}\text{cm}^{-1}$ ;  $\epsilon_{365\text{ nm}} = 0.00\text{ M}^{-1}\text{cm}^{-1}$ ;  $^1\text{H NMR}$  (60 MHz, NEAT)  $\delta$  7.25-7.81 (m, 3H), 5.91-7.23 (m, 3H); IR ( $\nu$ ,  $\text{cm}^{-1}$ ) 1752.1, 1636.1, 1214.3, 981.2, 895.0, 883, 796.9; MS ( $m/z$ ) 50, 55, 59, 75, 93, 117, 143, 172, 174, 226, 228, 281.

4-Iodophenyl Acrylate (3g).



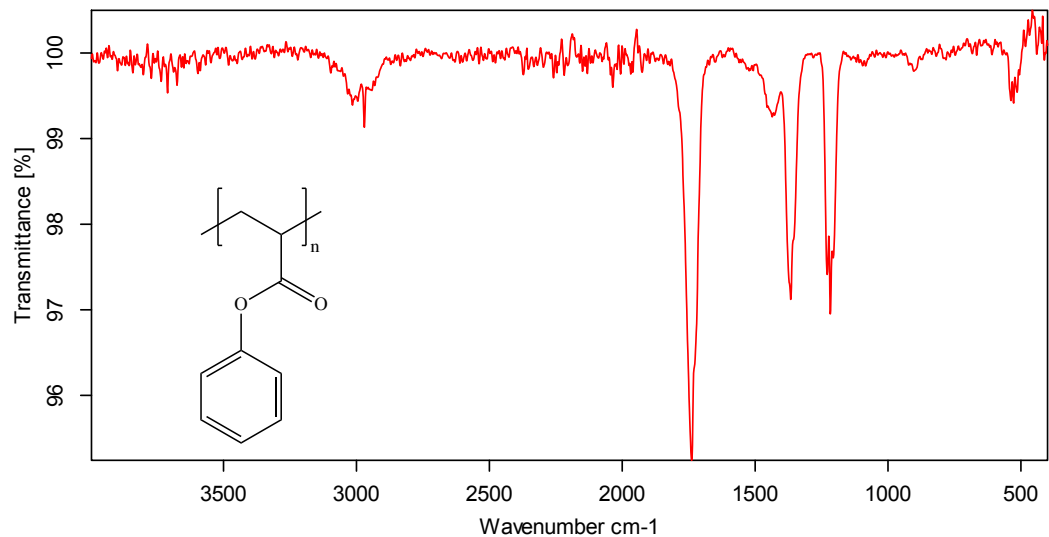
A pale yellow oil; average isolated yield < 10%;  $n_D^{25} = 1.5229$ ;  $\epsilon_{266\text{ nm}} = 3434.39\text{ M}^{-1}\text{cm}^{-1}$ ;  $\epsilon_{313\text{ nm}} = 0.00\text{ M}^{-1}\text{cm}^{-1}$ ;  $\epsilon_{365\text{ nm}} = 0.00\text{ M}^{-1}\text{cm}^{-1}$ ;  $^1\text{H NMR}$  (60 MHz, NEAT)  $\delta$  6.65-8.00 (m, 4H), 5.81-6.64 (m, 3H); IR ( $\nu$ ,  $\text{cm}^{-1}$ ) 1746.6, 1634.0, 1201.5, 981.5, 898.7, 802.3; MS ( $m/z$ ) 55, 58, 85, 98, 112, 127, 162, 207.

**Data S3. Product Characterization: Homopolymers of phenyl acrylate derivatives, Related to Table 3 and Figures 2-4.**

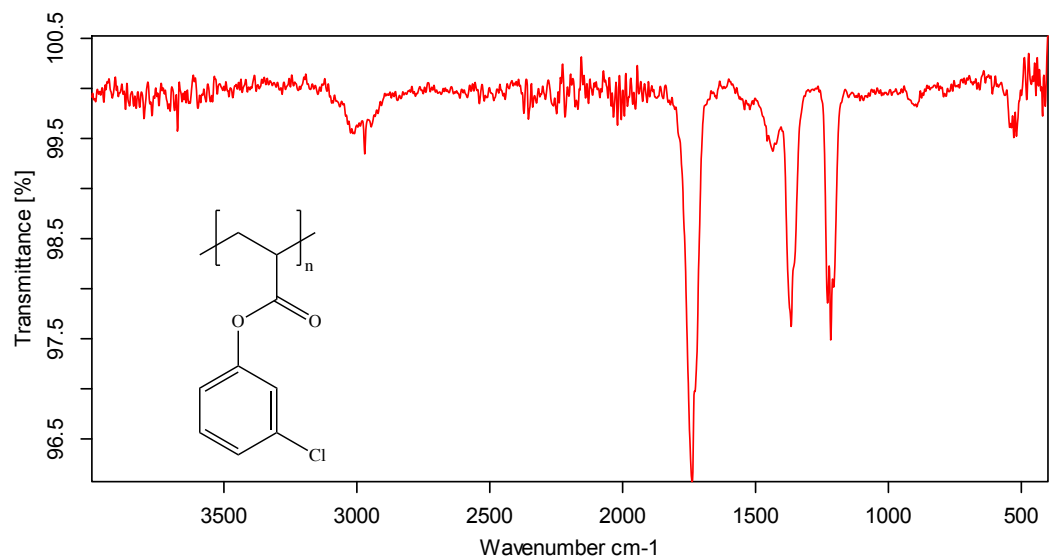
Upon polymerization, the homopolymers of the phenyl acrylate derivatives were analyzed via ATR-FT-IR. Each homopolymer was devoid of vinyl functionality evidenced by the absence of distinguishing vinylic peaks [IR ( $\nu$ ,  $\text{cm}^{-1}$ ) 1633, 984, 920]. Furthermore, the ATR-FT-IR was largely unchanged for the homopolymers over the course of three years when stored in a humidity controlled environment. In other

words, no degradation or delamination of the homopolymer coatings were observed after aging for three years.

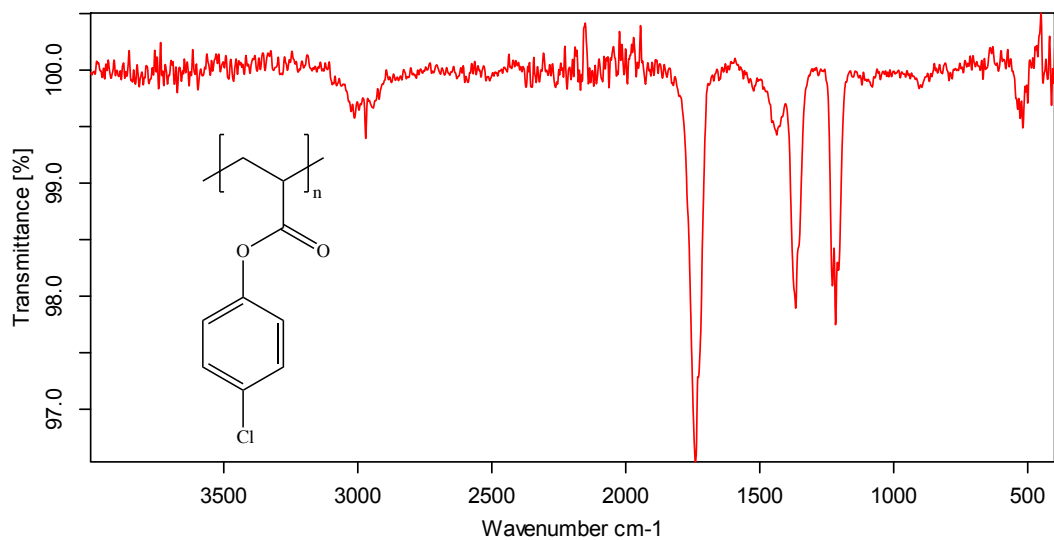
ATR-FTIR of poly(phenyl acrylate) ( $\nu$ ,  $\text{cm}^{-1}$ ) 3009, 2970, 1730, 1436, 1366, 1229, 1217, 1206, 903.



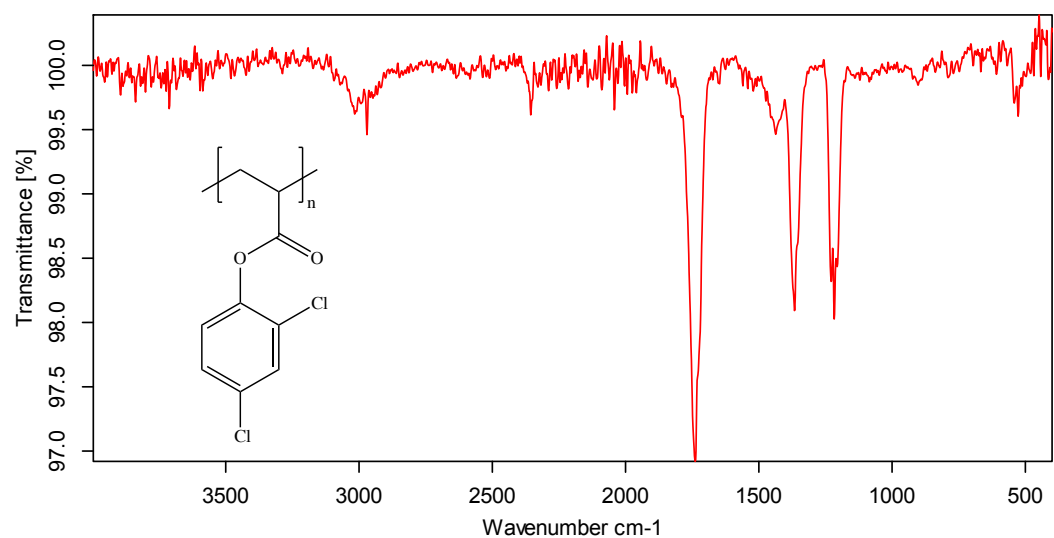
ATR-FTIR of poly(3-chlorophenyl acrylate) ( $\nu$ ,  $\text{cm}^{-1}$ ) 3009, 2970, 1738, 1435, 1366, 1229, 1217, 1206, 893.



ATR-FTIR of poly(4-chlorophenyl acrylate) ( $\nu$ ,  $\text{cm}^{-1}$ ) 3012, 2970, 1740, 1437, 1366, 1229, 1217, 1206, 905.

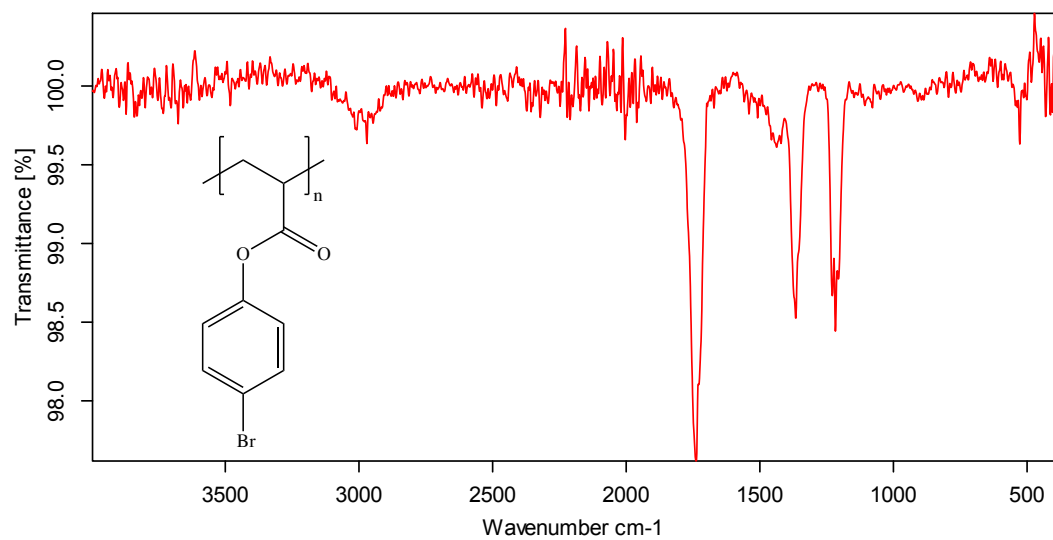


ATR-FTIR of poly(2,4-dichlorophenyl acrylate) ( $\nu$ ,  $\text{cm}^{-1}$ ) 3016, 2970, 1738, 1437, 1366, 1228, 1217, 1206, 903.

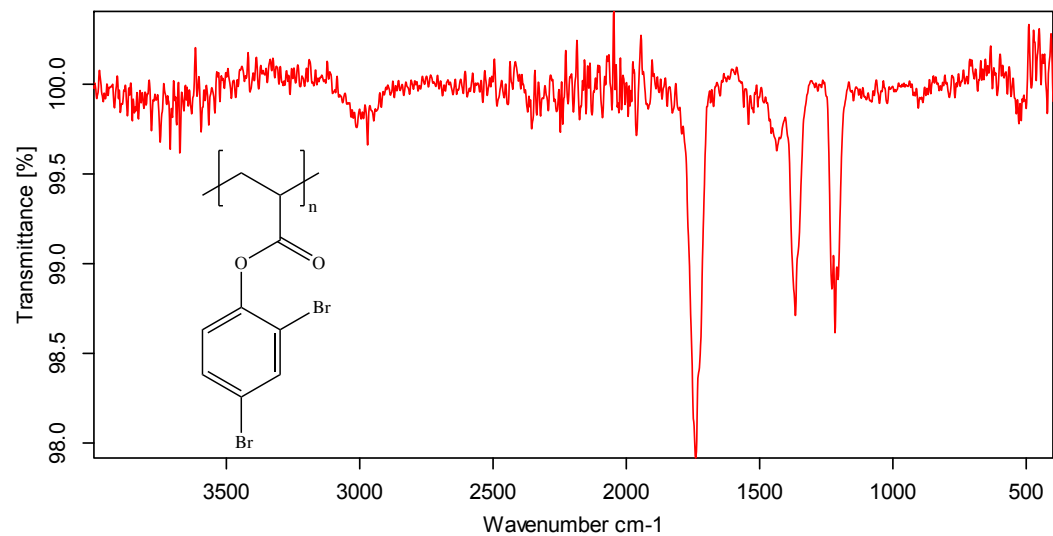




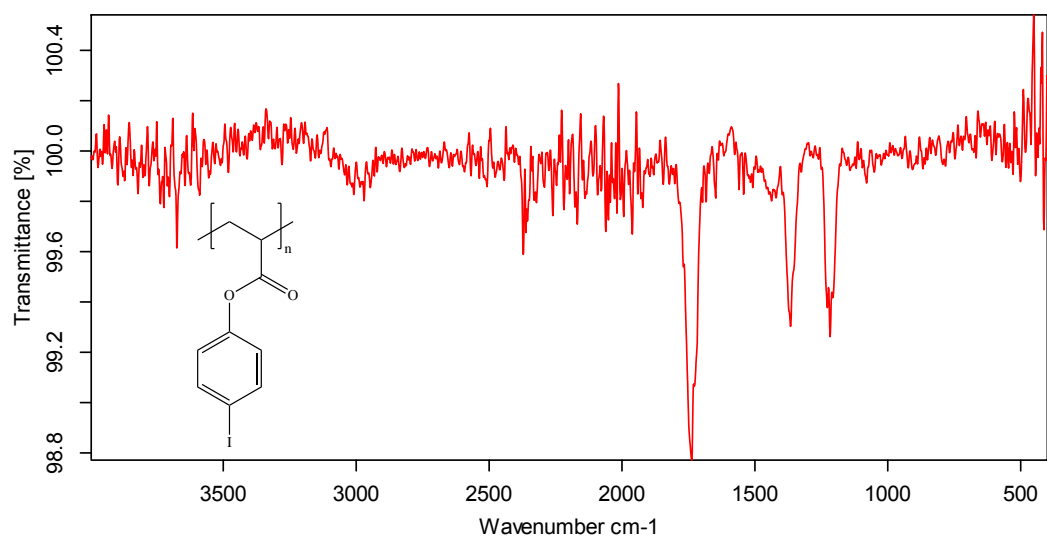
ATR-FTIR of poly(4-bromophenyl acrylate) ( $\nu$ ,  $\text{cm}^{-1}$ ) 3014, 2970, 1738, 1437, 1229, 1217, 1206, 909, 895.



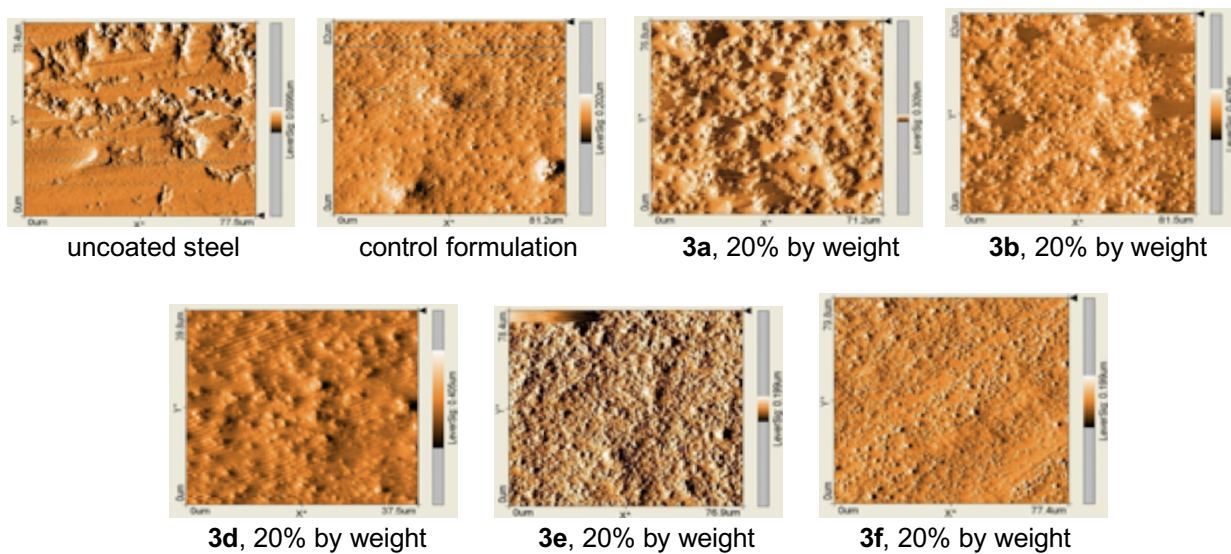
ATR-FTIR of poly(2,4-dibromophenyl acrylate) ( $\nu$ ,  $\text{cm}^{-1}$ ) 3011, 2970, 1740, 1436, 1366, 1228, 1217, 1206, 905, 898.





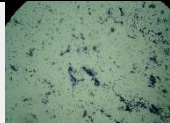
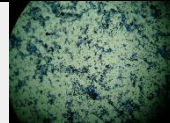
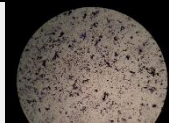

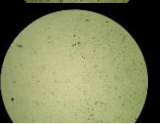
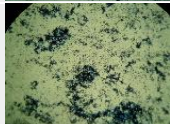


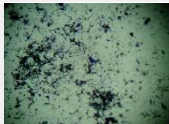
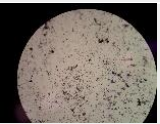
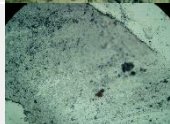
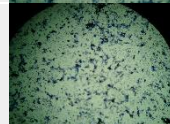
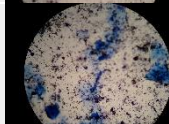
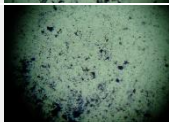

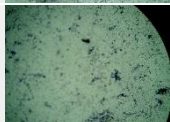
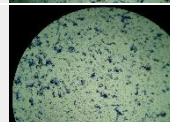
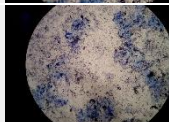
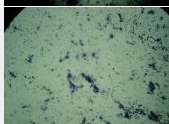
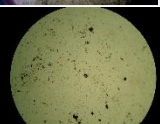
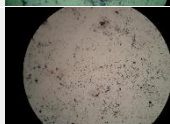

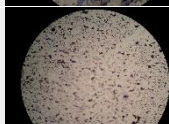
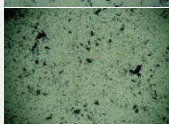

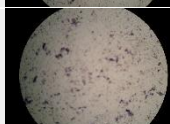
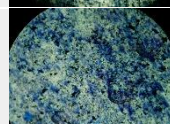
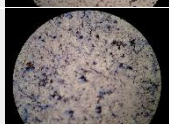
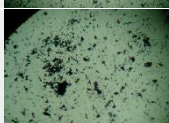
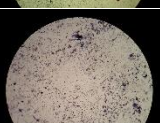
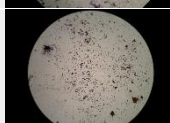
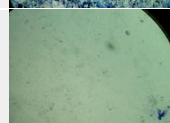
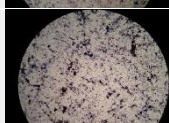
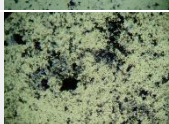
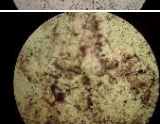
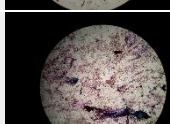

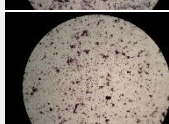
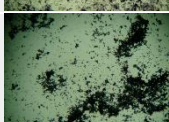
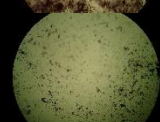
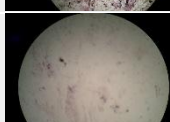
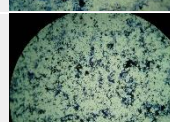
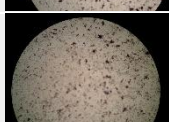
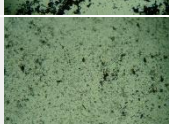
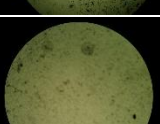

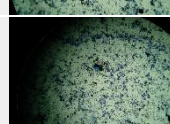
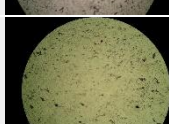
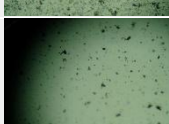
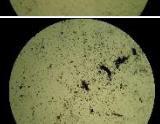
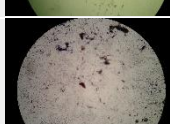
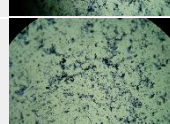
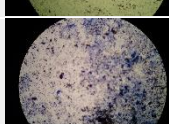
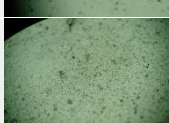
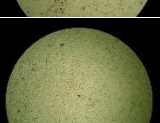
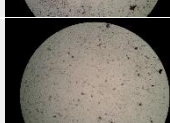
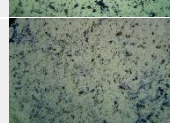
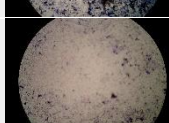
ATR-FTIR of poly(4-iodophenyl acrylate) ( $\nu$ ,  $\text{cm}^{-1}$ ) 3009, 2956, 1738, 1437, 1366, 1227, 1217, 1207, 907.



**Data S4. Figures associated with Transparent Methods.**



**Figure S1. AFM surface profile scans, contact scanning mode, Related to Table 2.**

Sample	<i>E. coli</i>	<i>S. aureus</i>	<i>P. aeruginosa</i>	<i>S. typhimurium</i>	<i>S. pneumoniae</i>
Control coating (uncoated)					
Control coating					
3a control (uncoated)					
3a					
3b control (uncoated)					
3b					
3d control (uncoated)					
3d					
3e control (uncoated)					
3e					
3f control (uncoated)					
3f					

**Figure S2. Stained plastic slides of representative monomers (i.e., 3a, 3b, 3d, 3e, and 3f) at 20 weight percent coating incorporation (100x magnification) after biofilm reactor incubation, Related to Figure 1.**

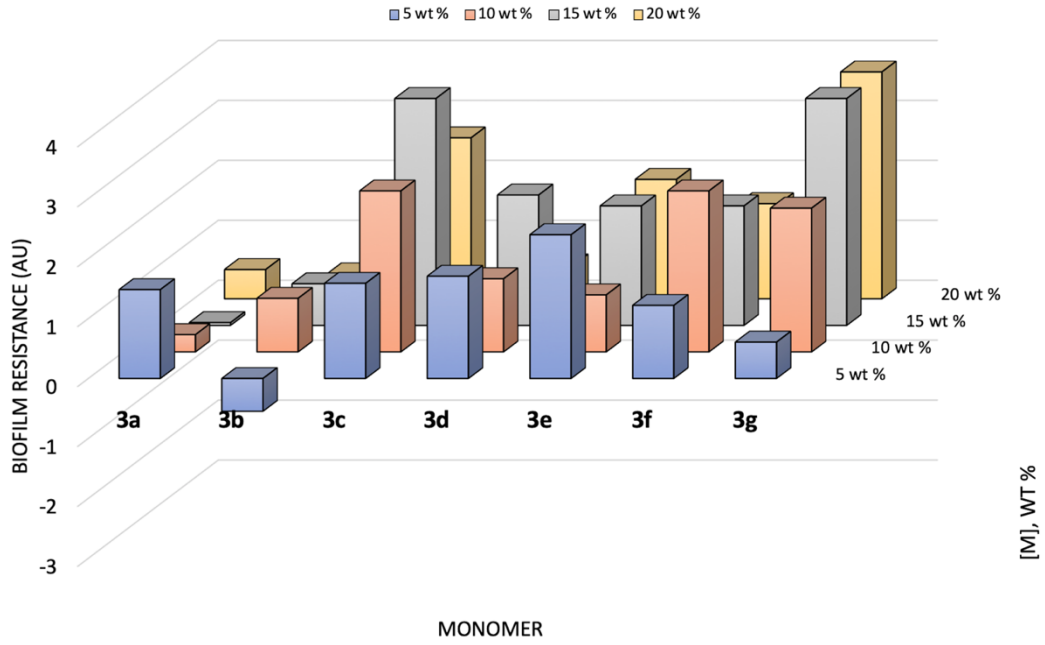


Figure S3. Evaluation of *E. coli* biofilm resistance, Related to Figure 1.

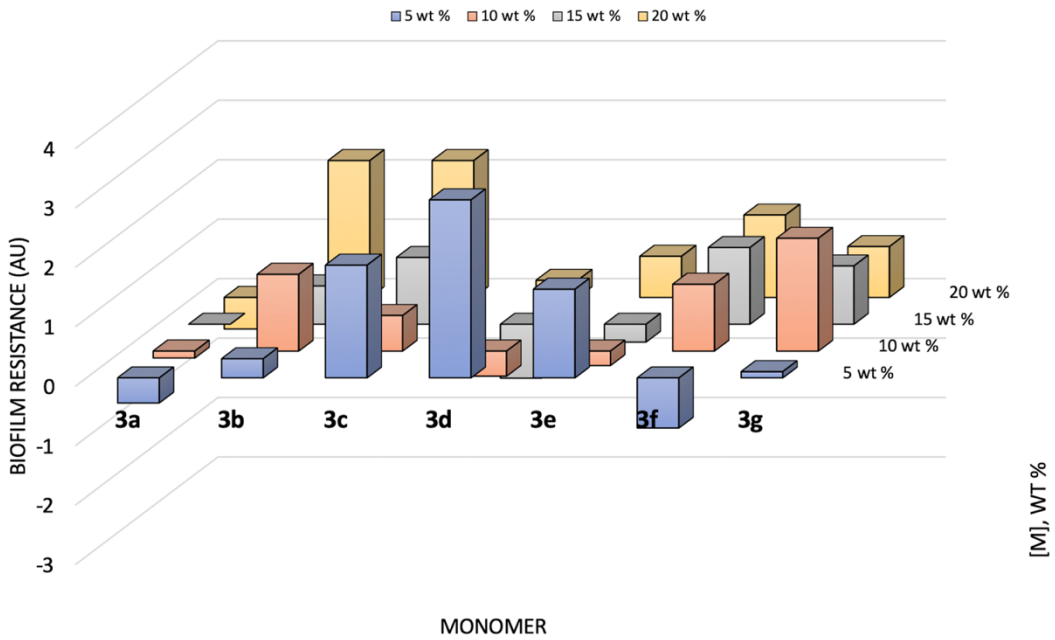


Figure S4. Evaluation of *P. aeruginosa* biofilm resistance, Related to Figure 1.

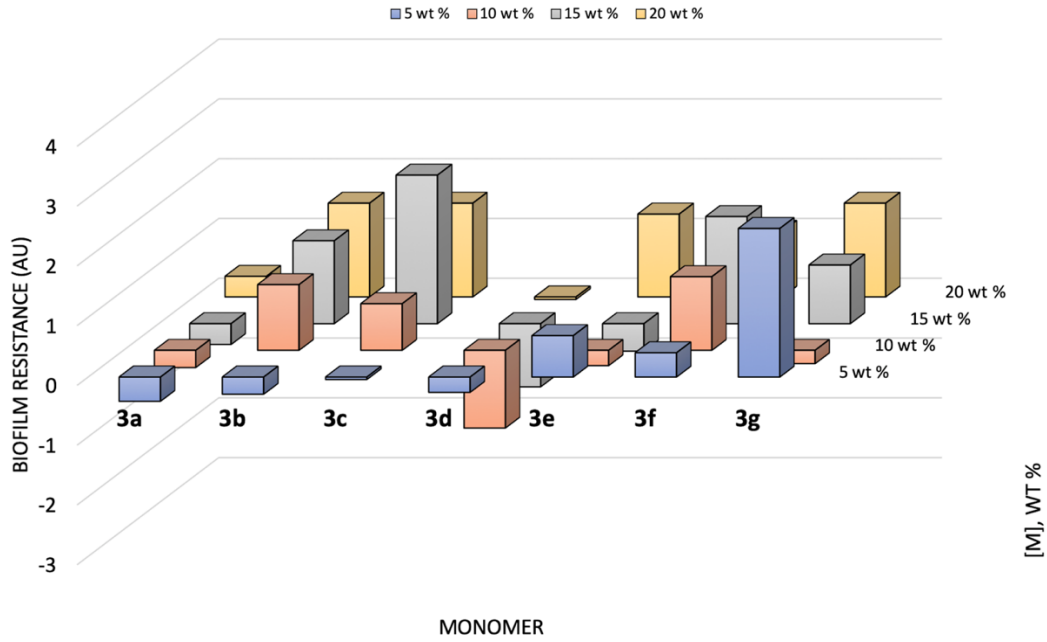


Figure S5. Evaluation of *S. aureus* biofilm resistance, Related to Figure 1.

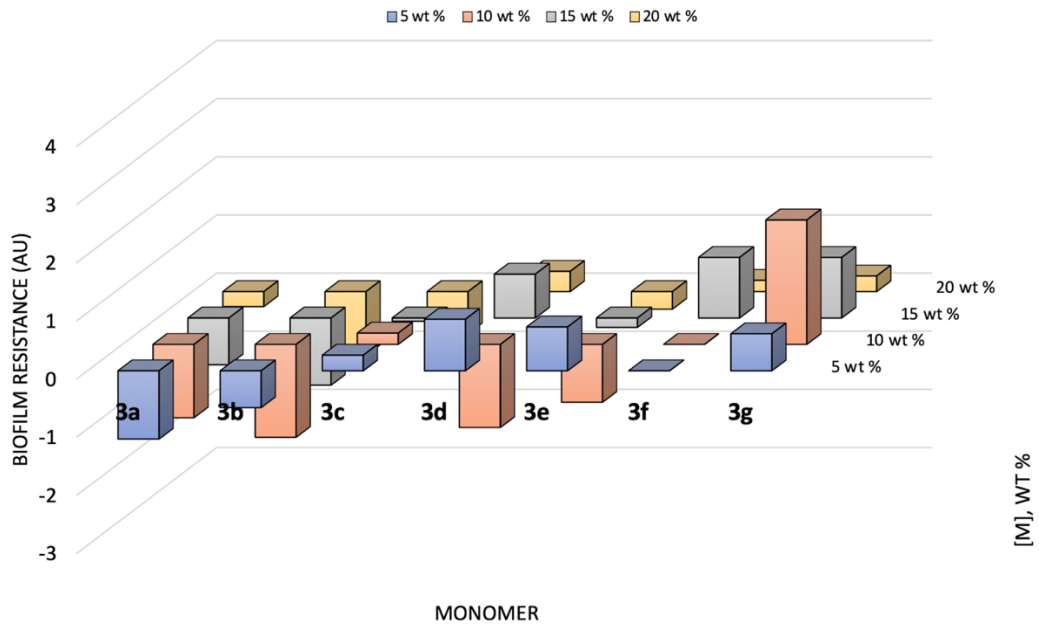


Figure S6. Evaluation of *S. pneumoniae* biofilm resistance, Related to Figure 1.



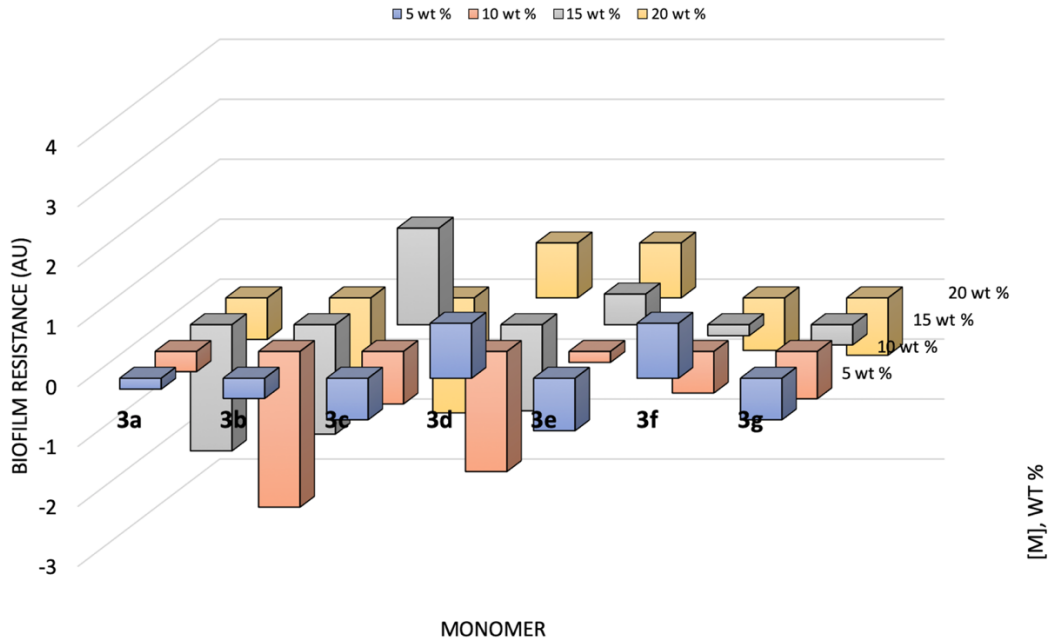


Figure S7. Evaluation of *S. typhimurium* biofilm resistance, Related to Figure 1.

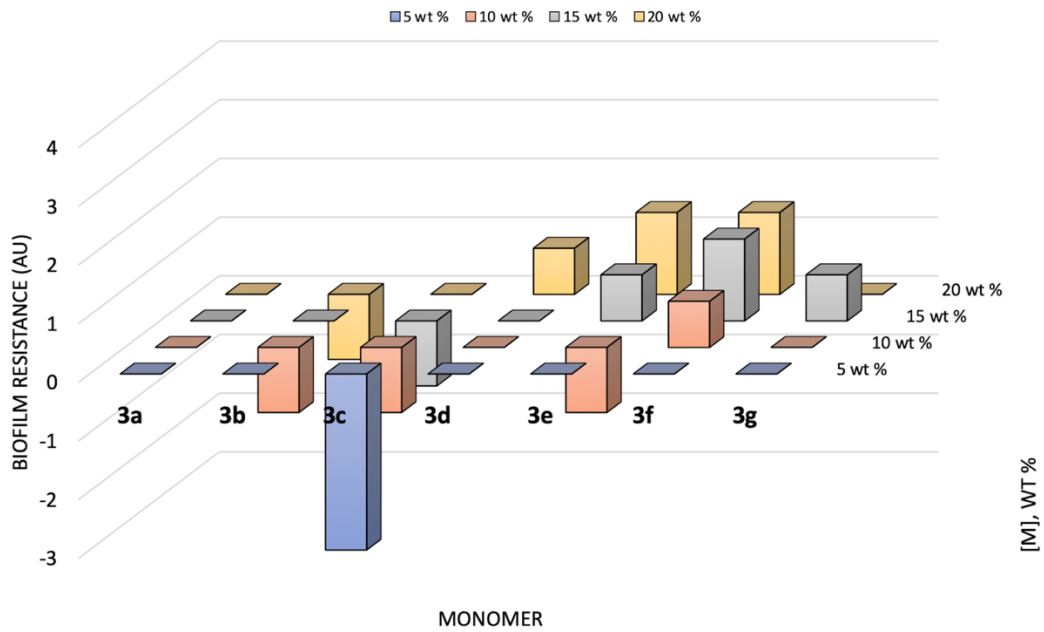


Figure S8. Qualitative evaluation of multiple species biofilm resistance in raw clarified sewage, Related to Figure 1.

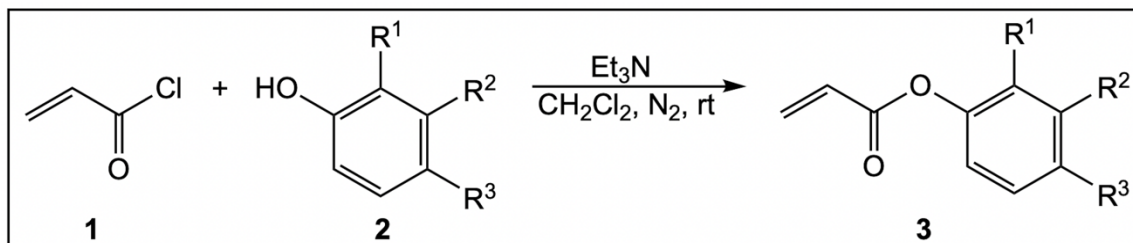


Figure S9. Synthetic reaction scheme, Related to Table 1.

## TRANSPARENT METHODS

### A. General Information

#### Materials and Instrumentation.

Most chemicals used in the monomer syntheses and testing, including the phenolic precursors, triethylamine (Et<sub>3</sub>N), acryloyl chloride, and acetonitrile, were purchased from Sigma-Aldrich. The dichloromethane also used in the syntheses was purchased from Pharmacia. The material used for the coating formulations was obtained from Allied Photochemical and is a proprietary formulation. Cytec Specialty Chemicals provided the 1,6-hexanediol diacrylate (HDODA) used in the photo-DSC. Albemarle Corporation donated the photoinitiator, 2,2-dimethoxy-2-phenylacetophenone (DMPA). The uncoated, polished stainless-steel plates were purchased from Q Panel Products. Methyl ethyl ketone (MEK) for the double rub test was purchased from The Paint Center. Cytology fixative spray was obtained from Andwin Scientific. Nitrogen gas was provided by Airgas.

The bacteria were stained using Hema-diff solution 3-thiazine dye from Anapath. Bacteria were obtained from Carolina Biological Supply. The Luria-Bertani, Miller (LB Miller) nutrient agar was provided by Fisher Scientific. The Trypticase Soy Agar and Bacto Blood Agar Base, Dehydrated were obtained from Difco. BBL SIM Medium was obtained from BBL Microbiology Systems.

Characterization of monomers and polymers was conducted using multiple machines. The NMR Spectrometer Eft-60 was provided by Anasazi Instruments Inc. The Infrared Spectrophotometer was obtained from Perkin Elmer (1600 Series). The rotary evaporator (Rotovap), collegiate model, was provided by Heidolph LABORTA. Sargent-Welch Scientific Company provided the Welch DuoSeal Vacuum Pump, Model 1400. Mel-Temp Electrothermal melting point apparatus (Model 1201D) was provided by Barnstead/Thermolyne. Refractometer was obtained from Thermo Electron Corporation (Model 334610). Photo-Differential Scanning Calorimeter (DSC 822<sup>e</sup>) was obtained from Mettler Toledo and the ultraviolet spot light source was the Lightningcure 200 by Hamamatsu. The Ultraviolet-Visible Spectrometer (HP 8453) was obtained from Hewlett-Packard. Light Microscope (Model M404DP) was provided by Swift Instruments International. AMSCO provided the autoclave model AMSCO 3021 Gravity. Incubation was performed in a GI200A-1 model incubator from Thermo Electron Corporation.

#### UV-Vis Spectroscopy.

10.0 mL acetonitrile was measured out in a graduated cylinder then added to scintillation vials containing 0.05 g of the monomer. UV-Vis spectra were taken of each monomer then diluted with acetonitrile as

necessary [until absorbance was measured between 0.75-1.0]. Measurements were taken of absorbance at specific wavelengths of the monomers using UV Vis and used to determine the extinction coefficient at wavelengths of 266, 313, and 365 nm.

### **Coating Production.**

*Application of Formulation to Unpolished Stainless-Steel Plates.* The plates and draw down bar were washed with acetone. The drawdown bar was set in the position demarking four mils (100  $\mu\text{m}$ ), and the formulation was applied to the plate along the top edge of the drawdown bar. The drawdown bar was then drawn at uniform speed to evenly apply the coating. If streaking or orange peel occurred, the drawdown was repeated until the formulation was evenly applied.

*Application of Formulation to Plastic Slides.* Six one-inch by three-inch (1 in. x 3 in.) plastic (optically clear vinyl) slides were prepared per coating formulation. Six slides were laid horizontally together to form a solid plastic surface with the sides taped down. The drawdown bar was placed on the slides and formulation was applied to the top-most slides. The drawdown bar was observed to be in the four mil position and drawn down at uniform speed to evenly coat half of the surface of each of the six slides. If streaking or orange peel occurred, the drawdown was repeated until the formulation was evenly applied.

*Application of Formulation to Glass Slides.* One, one-inch by three-inch (1 in. x 3in.) glass slide was prepared per formulation. Four glass slides were laid down vertically to form two columns of two slides each far enough apart to fit a fifth glass slide in the middle (the one to be coated) and to allow the edges of the draw down bar to rest on them. In this manner a uniform coating depth was achieved for the targeted glass slide because the drawdown bar rested not on the experimental surface, but on glass slides of the same size as the target. When the drawdown bar was placed on the supporting glass slides and observed to be in the four mil position, formulation was applied to the target glass slide. The drawdown bar was drawn at a uniform speed to spread the formulation evenly; however, if streaking or orange peel occurred, the drawdown was repeated.

*Polymerization of phenyl acrylate monomer derivatives.* Multiple passes under a Fusion UV Systems, Inc. LC-6/F300S equipped with a H-bulb cured the formulations (one weight percent DMPA dissolved in monomer) in air at 20 feet per minute and were confirmed via a traditional thumb-twist test. The coatings were cured to metal plates, plastic slides, and glass slides to conduct various physical and biological tests.

*Biologic sample preparation for contact angle measurements.* Bovine collagen (purchased from Aldrich) coatings were prepared according to established literature protocols (Hansen et al., 2011). For consistency, insoluble and soluble collagen concentrations were measured to be 100  $\mu\text{g}/\text{mL}$ . Soluble collagen was dissolved in a phosphate buffer system (1 x PBS, pH = 7.4) purchased from Aldrich.

Both *S. aureus* and *P. aeruginosa* were rehydrated according to established procedures from the supplier and transferred aseptically onto two 10 mL Luria-Bertani (LB), Miller, nutrient agar plates. The inoculated plates were placed in an incubator at 37°C for 72 hours. After incubation, the specimens were placed in a refrigerator and stored at 6°C until use.

### **Atomic Force Microscopy (AFM): Related to Table 2.**

Atomic force microscopy (AFM) contact scanning curves of each coating were obtained at two locations that were an approximate 80  $\mu\text{m}$  x 80  $\mu\text{m}$  area (6,400  $\mu\text{m}^2$ ) to eliminate the effects of interference on the roughness measurements. Both X and Y roughness calculations were averaged to yield the average three-dimensional surface roughness ( $R_a$ ) for each location (Equation S1) (Raposo et al., 2007).



$$R_a(M, N) = \frac{1}{NM} \sum_{x=1}^N \sum_{y=1}^M [z(x, y) - \bar{z}(x, y)] \quad (\text{S1})$$

Three locations were arbitrarily selected for each plate whereupon the roughness and peak-valley height ( $R_z$ ) were determined (Equation S2) (Raposo et al., 2007).

$$R_z = \frac{1}{n} (\sum_{i=1}^3 R_{p,i} + \sum_{i=1}^3 R_{v,i}) \quad (\text{S2})$$

The roughness values and peak-valley height for the three locations were then all averaged for an overall average plate roughness and average peak-valley height. The average peak-valley height was then compared to that of surgical grade steel ( $R_z \leq 1 \mu\text{m}$ ). Scans of both controls and cured copolymers at 20 weight percent monomer incorporation are shown in Figure S1.

### Extraction Studies.

Extraction studies were performed for all cured formulations at 20 weight percent active monomer incorporation using gas chromatography (GC) – mass spectrometry (MS). Each cured coating (0.5 g) was scraped from the steel plates, powdered, placed into 10 mL of methanol in a capped vial, and allowed to soak for one week at which point one milliliter of the supernatant was placed into a GC sample vial. The GC-MS was then run for each of the samples whereupon the percent extractables were calculated. The lower limit of detection is 100  $\mu\text{g/mL}$ . The GC used a 30 m (0.1 mm inside diameter) nonpolar column with a 250°C injection temperature, 150°C oven temperature, and 280°C interface temperature.

### Photo-Differential Scanning Calorimetry (Photo-DSC).

The monomers (i.e., phenyl acrylate derivatives, **3a-g**) were formulated at ten weight percent with one weight percent DMPA in HDODA, and then two microliters (2  $\mu\text{L}$ ) of each formulation was measured into crimped, aluminum sample pans. The light intensities were measured using black body absorbers. The calorimetric measurements were performed using a Mettler-Toledo DSC 822<sup>e</sup> modified with a Hamamatsu Lightning Cure 200 UV-spot, equipped with a full-arc high-pressure mercury lamp. The sample cell was kept at a constant 20°C by a Julabo FT 100 intercooler. The sample was purged with nitrogen for two minutes prior to beginning the run and continued through the completion of the run. The polymerization rates of each monomer were compared to that of NEAT HDODA and to a HDODA sample photoinitiated by a standard *Norrish Type I* photoinitiator (e.g., DMPA). No increased polymerization rate for all samples indicate persistence of the aryl halide in the final polymerized sample.

### Single Species Biofilm Resistance Studies: Related to Figure 1.

The ability of microorganisms to form biofilms on the coatings was tested through the cultivation of five different bacteria and subsequent exposure of these microorganisms to the coatings.

*Cultivation.* All specimens were rehydrated according to established procedures from the supplier. The rehydrated bacteria (*Escherichia coli*, *Staphylococcus aureus*, *Salmonella typhimurium*, and *Pseudomonas aeruginosa*) were transferred aseptically into four test tubes containing 10 mL LB, Miller, nutrient agar slants. The inoculated test tubes were placed in an incubator at 37°C for 72 hours. After incubation, the specimens were placed in a refrigerator and stored at 6°C until use.

*Streptococcus pneumoniae* was cultivated within an agar composed of 45% Trypticase™ Soy Agar, 30% Blood Base Agar, and 25% BBL SIM agar. Due to the fastidious nature of *S. pneumoniae*, *S. pneumoniae* was the only specimen cultivated anaerobically in six plates composed of 10mL each of the aforementioned

custom agar and in four test tube slants containing 10 mL of the custom agar. The inoculated samples were placed in an incubator at 37°C for 72 hours and afterward stored in a refrigerator at 6°C.

*Induction of Biofilm Formation.* A biofilm reactor was built to characterize the biofilm resistance of coatings within a bacteria rich environment. A fish tank (30 inches in length, 12.25 inches wide, and 12.5 inches high) was divided into five equally sized sections using custom cut poly(methyl methacrylate) sheets and sealed with waterproof sealant to prevent cross contamination. An evaporative cooler pump was placed in each compartment to circulate approximately three liters of bacterial broth in each compartment. The solution was composed of 3000 mL sterilized water with three grams of LB, Miller, nutrient agar. Each bacterial strain was cultivated in 100 mL of water and 0.3 g of LB, Miller, nutrient agar at 37°C for 24 hours. After 24 hours the inoculated broths were poured into corresponding sections of the biofilm reactor. Plastic slides containing each of the coating formulations were simultaneously placed in the reactor on a holding apparatus built to allow for a flow assay to measure biofilm growth. In other words, biofilm growth was performed in bulk upon every sample simultaneously. Each plastic slide was divided into an uncoated side (internal control) and a coated side (measuring biofilm growth). Over the course of 10 days, 500 mL of broth was replaced with 500 mL sterilized water each day. After this 10 day period, the holding apparatus and all slides were removed as one. The unattached bacteria and any other materials were rinsed from the slides with sterile, deionized water. The slides were sprayed with a cytology fixative [poly(ethylene glycol)-based]. After the fixative was air dried, the slides were rinsed with deionized water, and stained with methylene blue/Azure A. The excess dye was removed with sterile water leaving behind any residual stained bacteria on the slide. Representative stained samples are provided in Figure S2.

Upon cultivating single species biofilms in the custom-built biofilm reactor, qualitative examination of coated plastic slides was performed via optical microscopy (100x magnification) to ascertain success of the biofilm resistant polymers after staining. Quantitative evaluation of the biofilm resistance of the phenyl acrylate monomers relative to the bacterium were determined via colony forming unit (CFU) count. All CFU counts are relative to the control coating with no phenyl acrylate monomer derivatives present (Figures S3-S7 scaled identically).

Figures S3-S7 are quantitatively normalized relative to biofilm growth on the control coating [i.e., UV-curable semi-gloss acrylic clearcoat (Allied Photochemical, KZ-7025-CL)]. Reduced biofilm resistance relative to the control is negative while increased biofilm resistance is positive. Biofilms for Figures S3-S5 and S7 were cultured for 10 days at 38°C in LB Miller agar broth under starvation conditions. Likewise, the biofilm related to Figure S6 was cultured; however, the broth used was a blood-based soy agar.

Some biofilm resistance was observed for monomers **3c-g**; however, monomers **3a** and **3b** did not exhibit any appreciable *E. coli* biofilm resistance. While the lack of biofilm resistance for **3a** was expected, that of **3b** might indicate that *meta*-chlorination promotes limited biofilm resistance toward *E. coli*. Some biofilm resistance was observed for **3d**. With a direct relationship of monomer concentration to biofilm resistance, **3c**, **3f**, **3e**, and **3g** demonstrated significant biofilm resistance. Also, *para*-halogenation seems to increase biofilm resistance for *E. coli*. The heavier brominated and iodinated monomers were generally better biofilm inhibitors than the chlorinated derivatives.

*P. aeruginosa* is among the best biofilm forming bacteria and was a logical choice for demonstrating biofilm resistance. The chlorinated monomers (**3b**, **3c**, and **3d**) exhibited more significant biofilm resistance to *P. aeruginosa* than the brominated or iodinated monomers. However, at higher concentrations of the brominated (**3e** and **3f**) or iodinated (**3g**) monomers, biofilm resistance increased. Interestingly, **3d** was more efficacious at lower concentrations indicating that the biostatic effect inherent to a MIC may be a more important effect for this bacterium than ensuring a cidal effect via MBC.

The monochlorinated monomers (**3b** and **3c**), especially at increased concentrations, inhibited biofilm development of *S. aureus*; yet, **3d** did not exhibit appreciable biofilm resistance. At increasing concentrations of the brominated monomers (**3e** and **3f**), biofilm resistance increased noticeably indicating a direct concentration correlation. Both **3e** and **3g** had a biostatic effect similar to that previously described for **3d** with *P. aeruginosa*.

Across the board, less biofilm resistance was observed for the monomers toward *S. pneumoniae* lower monomer concentrations ( $\leq 15$  weight percent) did not inhibit biofilm formation. Three derivatives (e.g., **3d**, **3f**, and **3g**) exhibited moderate biofilm resistance with **3g** being most effective. Again **3e** showed a biostatic effect. Multihalogenated monomers and softer atoms (e.g., bromine and iodine) seem to be most effective at inhibiting *S. pneumoniae* biofilm formation.

Moderate biofilm inhibition was observed for the 15 weight percent concentration of **3c**. *S. typhimurium* biofilms were most inhibited by the dichlorinated (**3d**) and monobrominated (**3e**) monomers at several concentrations. **3f** had a slight biostatic effect at low concentration. No clear trend was observed for biofilm inhibition of *S. typhimurium*.

### Multiple Species Biofilm Resistance Studies.

A multiple species biofilm resistance study for each coating was performed by immersion into sedimented (i.e., clarified) raw sewage in the secondary clarifiers at the Abilene Wastewater Reclamation Plant in Abilene, Texas.

Each cured slide was hot glued to a poly(methyl methacrylate), PMMA, sample sheet obtained from a local home improvement store. The sample sheet was placed into another custom-built apparatus resembling a metal cage, termed the biofilm resistance apparatus (BRApp), in order to protect the samples from mechanical processes that could remove either the coating or the grown biofilm.

Then, the BRApp was taken to the Abilene Wastewater Reclamation Plant and submerged into the secondary clarifier which allows the aerated raw sewage to grow existing microbes, some of which consume a portion of the raw sewage materials. It is important to note that the bulk of the solid sewage was removed via sedimentation in the primary clarifiers prior to aeration. Each secondary clarifier is capable of handling 1.75 million gallons of raw sewage each day. The BRApp was left in the secondary clarifier for two days (3.5 million gallons of total exposure) at about a six foot depth, just above the paddle arm that mixes the contents at a rate of six revolutions per hour and ambient outside temperature.

The BRApp was removed and transported back to the lab in a plastic bag whereupon the PMMA sheet was removed, rinsed with deionized water, and treated with an ethanol spray to kill the microbes attached to the sheet and samples. The microbes were then fixated with a poly(ethylene glycol) cytological spray and allowed to dry. Then the slides were stained with a methylene blue/Azure A solution. Each stained slide was qualitatively evaluated by comparing each coating relative to the uncoated portion of the slide both with the naked eye and through an optical microscope (100x) in three different locations on the coating and scaled accordingly [e.g., scale: 1 (excessive biofilm) – 3 (same as control) – 5 (minimal biofilm)]. Data are aggregated in Figure S8 which was qualitatively normalized relative to biofilm growth on the control coating [i.e., UV-curable semi-gloss acrylic clearcoat (Allied Photochemical, KZ-7025-CL)]. Reduced biofilm resistance relative to the control is negative while increased biofilm resistance is positive.

Similar to the laboratory-based, single bacterium studies and after exposure to 3.5 million gallons of raw clarified sewage, the coatings incorporating the brominated monomers (**3e** and **3f**) were most efficacious as biofilm resistant materials. Likewise, the dihalogenated (**3d** and **3f**) compounds seemed to also be more effective biofilm resistant monomers than the monohalogenated monomers of which **3g** exhibited some biofilm resistance unlike the monochlorinated monomers (**3b** and **3c**).

## B. Representative Procedures

### General Procedure for Synthesis of 3: Related to Table 1.

The phenolic derivative was dissolved in a slight molar excess of triethylamine (TEA) and then added to a 250 mL round bottom flask with 40 mL dichloromethane. Acryloyl chloride (equimolar amount compared to TEA) was added dropwise to the mixture with stirring (Table 1). After the flask was provided with a nitrogen atmosphere the mixture was stirred for 24 hours and thereafter suction filtered to remove the TEA hydrochloride salt. The resulting solution was washed in a separatory funnel 15 times with 15 mL deionized water then anhydrous magnesium sulfate ( $\text{MgSO}_4$ ) was added until clumping stopped. The mixture was suction filtered to remove the anhydrous  $\text{MgSO}_4$  and thereafter placed on the Rotovap for solvent volume reduction. The remaining liquid acrylate was dried via vacuum for 24 hours. The reaction scheme is provided in Figure S9.

NOTE: **3g** was a difficult synthesis and required multiple scaled-up reactions to acquire an adequate amount of the compound for testing; therefore, the corresponding reported average isolated yield is low and not comparative to the other syntheses.

### C. Surface Energy Calculations: Related to Tables 3 and 4 and Figures 2-4

While surface energy analyses have many forms, we have chosen one that is arguably the simplest analyses and has historically been used to describe biological systems (Owens et al., 1969; Schrader, 2002; van Oss et al., 1987; van Oss et al., 1988). According to Equation S3, the change in Gibbs energy of an interface ( $\Delta G_{interface}$ ) is directly related to the surface energy of an interacting material ( $\gamma_m$ ) (van Oss et al., 1988).

$$\Delta G_{interface} = (1 + \cos \theta_{interface})\gamma_m \quad (\text{S3})$$

Equation S4 defines  $\gamma_m$  (generically represented as  $\gamma^{tot}$ ) to be the sum of the material's individual nonpolar ( $\gamma^{LW}$ ) and polar ( $\gamma^{AB}$ ) components where  $\gamma^{AB}$  is defined to be the geometric mean of the separate acid ( $\gamma^+$ ) and base ( $\gamma^-$ ) components (Equation S5) (van Oss et al., 1988).

$$\gamma^{tot} = \gamma^{LW} + \gamma^{AB} \quad (\text{S4})$$

$$\gamma^{AB} = 2\sqrt{\gamma^+\gamma^-} \quad (\text{S5})$$

Using two fully characterized liquid materials, the Owens-Wendt equation (S6) allows the determination of multiple surface energy components of a substrate (e.g.,  $\gamma_s^{LW}$ ,  $\gamma_s^{AB}$ , and  $\gamma_s$ ) via contact angle ( $\theta_{sl}$ ) (Owens et al., 1969; Schrader, 2002).

$$(1 + \cos \theta_{sl})\gamma_l^{tot} = 2\left(\sqrt{\gamma_s^{LW}\gamma_l^{LW}} + \sqrt{\gamma_s^{AB}\gamma_l^{AB}}\right) \quad (\text{S6})$$

The van Oss-Chaudhury-Good (OCG) equation (S7) expands Equation S6 to similarly delineate the substrate's separate acid ( $\gamma_s^+$ ) and base ( $\gamma_s^-$ ) components using three fully characterized liquids. Both  $\gamma_s^{AB}$  and  $\gamma_s$  can be determined sequentially via Equations S4 and S5 (van Oss et al., 1987; van Oss et al., 1988).

$$(1 + \cos \theta_{sl})\gamma_l^{tot} = 2\left(\sqrt{\gamma_s^{LW}\gamma_l^{LW}} + \sqrt{\gamma_s^+\gamma_l^-} + \sqrt{\gamma_s^-\gamma_l^+}\right) \quad (\text{S7})$$

Using a linear algebraic method to simultaneously solve for components, we used Equation 1 to determine the surface energy profile (e.g.,  $\gamma_s^{LW}$ ,  $\gamma_s^{AB}$ ,  $\gamma_s^+$ ,  $\gamma_s^-$ , and  $\gamma_s$ ) of each polymerized halogenated monomer.

### Contact angle measurements.

The sessile drop method was utilized where a 2  $\mu\text{L}$  droplet was placed on a surface and allowed to equilibrate for one minute. Following equilibration, the drop was photographed using a mounted second generation iPad Mini equipped with a macrolens. Contact angle measurements were obtained via a protractor app (Photo Protractor). To maintain quality control, the contact angle photographs were printed and secondarily validated manually via a physical protractor. Statistical averages for each contact angle measurement ( $N \geq 8$ ) were obtained after omitting the statistical outliers. We used bromonaphthalene, dimethylsulfoxide, formamide, and/or water to obtain contact angles used to determine the surface energy profiles.

### Linear algebraic determination of surface energy profiles.

A linear algebraic approach could be used to solve Equation S7 as given below using the complete characterization of the solvents used. After obtaining the contact angle measurements, Equation S8 was rearranged to yield Equation S8:

$$\frac{1}{2}[(1 + \cos \theta_{sl})\gamma_l^{tot}] = \sqrt{\gamma_l^{LW}\gamma_s^{LW}} + \sqrt{\gamma_l^-\gamma_s^+} + \sqrt{\gamma_l^+\gamma_s^-} \quad (\text{S8})$$

We then represent the experimentally determined or known values as  $a$ ,  $b$ ,  $c$ , and  $d$  and the unknown substrate values as  $x$ ,  $y$ , and  $z$  (Equation S9).

$$d = (a \cdot x) + (b \cdot y) + (c \cdot z) \quad (\text{S9})$$

where the corresponding contact angle measurement for a peculiar liquid is related to its characterized surface energy profile. Furthermore,  $d$  is defined to be  $\frac{1}{2}[(1 + \cos \theta_{sl})\gamma_l^{tot}]$ ,  $a$  is  $\sqrt{\gamma_l^{LW}}$ ,  $x$  is  $\sqrt{\gamma_s^{LW}}$ ,  $b$  is  $\sqrt{\gamma_l^-}$ ,  $y$  is  $\sqrt{\gamma_s^+}$ ,  $c$  is  $\sqrt{\gamma_l^+}$ , and  $z$  is  $\sqrt{\gamma_s^-}$ . We can now combine all values in matrix form.

$$\begin{array}{l} \text{bromonaphthalene} \\ \text{formamide OR dimethylsulfoxide} \\ \text{water} \end{array} \begin{array}{l} \left| \begin{array}{l} d \\ h \\ l \end{array} \right| = \left| \begin{array}{ccc} a & b & c \\ e & f & g \\ i & j & k \end{array} \right| \cdot \left| \begin{array}{l} x \\ y \\ z \end{array} \right| \end{array}$$

The 3x1 vector  $dhl$  (i.e.,  $d$ ), 3x3 matrix (i.e.,  $A$ ), and 3x1 vector  $xyz$  (i.e.,  $x$ ) can then be represented more simply as Equation S10.

$$d = A \cdot x \quad (\text{S10})$$

After performing an allowed matrix inversion, we can solve for  $x$  which gives us values for the substrate's heretofore unknown surface energy components:  $\gamma_s^{LW}$ ,  $\gamma_s^+$ , and  $\gamma_s^-$  (Equation S11).

$$x = A^{-1} \cdot d \quad (\text{S11})$$

Using the calculated component values, the substrate's acid-base component ( $\gamma_s^{AB}$ ) and overall surface energy ( $\gamma_s$ ) can be determined using Equations S5 and S4, respectively.

### SUPPLEMENTAL RESOURCES

Hansen, R. R.; Tipnis, A. A.; White-Adams, T. C.; Di Paola, J. A.; Neeves, K. B. (2011). Characterization of Collagen Thin Films for von Willebrand Factor Binding and Platelet Adhesion. *Langmuir*. 27, 22, 13648-13658.

Owens, D.; Wendt, R. Estimation of the Surface Free Energy of Polymers. (1969). *J. Appl. Polym. Sci.* 13, 1741-1747.

Raposo, M.; Ferreira, Q.; Ribeiro, P. A. (2007). A Guide for Atomic Force Microscopy Analysis of Soft Condensed Matter. In *Modern Research and Educational Topics in Microscopy*, A. Méndez-Vilas and J. Díaz, eds. (FORMATEX). 758-769.

Schrader, M. E. (2002). Young-Dupré Revisited. *Langmuir*. 11, 9, 3585–3589.

van Oss, C. J.; Chaudhury, M. K.; Good, R. J. (1987). Monopolar Surfaces. *Adv. Colloid Interface Sci.* 28, 35-64.

van Oss, C. J.; Good, R. J.; Chaudhury, M. K. (1988). Additive and Nonadditive Surface Tension Components and the Interpretation of Contact Angles. *Langmuir*. 4, 4, 884-891.